COMPUTING NONLINEAR AIRFOIL CHARACTERISTICS OF HELICOPTER ROTOR BLADES

Constantin ROTARU, Mihai Andres-MIHĂILĂ, Pericle Gabriel MATEI, Amado ŞTEFAN

Military Technical Academy, Bucharest, Romania

Abstract: *This paper deals with analytical and numerical study of helicopter rotor blades air loads, a subject which comes under the more general purpose of aerodynamic response (lift and pitching moment) for unsteady effects found on airfoil operating under nominally attached flow conditions away from stall. In this paper are presented some results about the study of air loads of the helicopter rotor blades, the aerodynamic characteristics of the airfoil sections, the physical features and the techniques for modeling the motion of the airfoil in the high angle of attack regime. The unsteady problem was approached on the basis of Theodorsen theory, where the aerodynamic response is considered as a sum of no circulatory and circulatory parts. The numerical calculus and the graphical parts were made in MAPLE software environment.*

Keywords: *unsteady aerodynamics, helicopter aerodynamics, rotor blade air loads*

1. INTRODUCTION

The aerodynamic behavior of airfoils in the high AoA regime is important for predicting the adverse effects produced in the reverse flow regime on the rotor. In the reverse flow region, the direction of the relative flow vector changes from the trailing edge toward the leading edge of the airfoil. While the fundamental process of the blade wake and tip vortex formation is similar to that found with a fixed wing, one difference with helicopter tip vortices is that they are curved and so they experience a self-induced effect. Another complication with helicopter rotors is that the wakes and tip vortices from other blades can lie close to each other and to the plane of blade rotation and so they have large induced effects on the blade lift distribution. Some authors have examined the higher harmonics of the rotor loading in forward flight and have concluded that the effects of the tip vortices are generally more important than the shed wake.

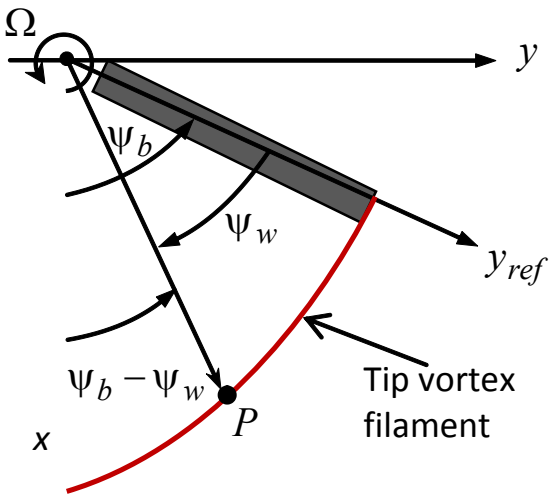

Fig. 1 Tip vortex trajectory

If the wake is assumed to be undistorted in the tip path plane and no wake contraction occurs in the radial direction (fig. 1), then the tip vortex trajectories are described by the equations

$$\begin{cases} x = R\cos(\psi_b - \psi_w) + R\,\mu\,\psi_w \\ y = R\sin(\psi_b - \psi_w) \end{cases} \quad (1)$$

where ψ_b is the position of the blade when the vortex was formed and ψ_w is the position of the vortex element relative to the blade.

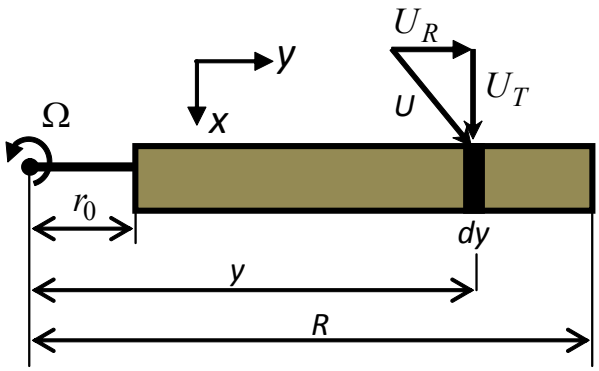

Fig. 2 Helicopter rotor blade

The angular or rotational speed of the rotor is denoted by Ω, the rotor radius by R, the advanced ratio $\mu = V_\infty \cos\alpha / \Omega R$ and $r = y / R$ where y is the axis along the rotor blade and α is the angle between the helicopter forward velocity V_∞ and the plane of the rotor. The subscript symbols T and R denote the tangential and radial velocity (fig. 2).

These interactions of blades and tip vortices (called blade-vortex-interactions, BVIs) can occur at many different locations over the rotor disk and also with different orientations.

The most important component of the helicopter is the main rotor for which there is a great deal of activity in developing new and improved mathematical models that predict the flow physics. A high tip speed gives the rotor a high level of stored rotational kinetic energy and reduces the rotor torque required for a given power, but there are two important factors that work against the use of a high tip speed: compressibility effects and noise.

The additional effects of compressibility on the overall rotor profile power requirements, when the tip of the advancing blade approaches and exceeds the drag divergence Mach number were estimated using the blade element theory combined with the airfoil section characteristics. A more detailed analysis of compressibility effects on the rotor must represent the actual nonlinear airfoil characteristics as functions of Mach number through stall at each blade element followed by numerical integration.

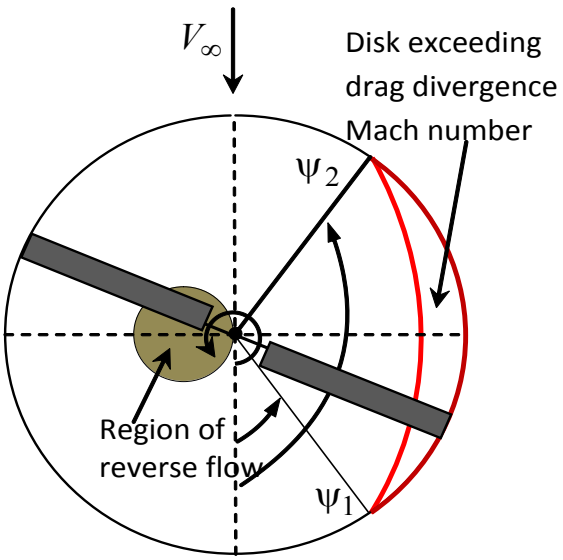

Fig. 3 Helicopter rotor in forward flight

The region of the rotor disk affected by compressibility effects is shown in fig. 3 and is defined on the surface where the incident Mach number of the flow that is normal to the leading edge of the blade exceeds the drag divergence Mach number, M_{dd}. If $M_{\Omega R}$ is the hover tip Mach number, than the region of the disk affected by compressibility effects is defined by

$$M_{r,\psi} = M_{\Omega R}(r + \mu \sin\psi) \geq M_{dd} \tag{2}$$

The azimuth angle for the onset drag divergence, ψ_1, can be obtained by setting $r = 1$, so that

$$\psi_1 = \arcsin\left(\left[\frac{1}{\mu}\left(\frac{M_{dd}}{M_{\Omega R}} - 1\right)\right]\right) \tag{3}$$

and $\psi_2 = 180 - \psi_1$.

The increment in the profile power ΔC_P associated with this region on the disk is

$$\frac{\Delta C_P}{\sigma} = \frac{1}{4\pi}\int_{\psi_1}^{\psi_2}\int_{r_{dd}}^{1}(r + \mu\sin\psi)^3 \Delta C_d \, r \, dr \, d\psi \tag{4}$$

where ΔC_d is the extra drag on the blade section when it exceeds the drag divergence Mach number, M_{dd} and σ is rotor solidity coefficient which represents the ratio of the blades area to the rotor disk area. For the NACA 0012 airfoil, Prouty (1986) suggests that this can be approximated by

$$\Delta C_d(M) = \begin{cases} 12.5(M-0.74)^3 & \text{for } M \geq 0,74 \\ 0 & \text{otherwise} \end{cases}$$

The rotor limits may be determined by two conditions, one condition given by advancing blade compressibility effects and the other one condition given by retreating blade stall. In either case the advancing blade operates at low angle of attack (AoA) but at high subsonic or transonic conditions, whereas the retreating blade operates at low Mach numbers and high lift coefficients.

The helicopter rotor airfoil must assure a high maximum lift coefficient, a high drag divergence Mach number, a good lift-to-drag ratio over a wide range of Mach number and a low pitching moment. At higher angles of attack the advert pressure gradients produced on the upper surface of the airfoil result in a progressive increase in the thickness of the boundary layer and cause some deviation from the linear behavior of lift versus angle of attack. On many airfoils, the onset of flow separation and stall occur gradually with increasing angle of attack, but on some airfoils (those with sharp leading edges) the flow separation may occur suddenly.

2. THE APPARENT MASS TENSOR

The rate of change of the impulse vector, in general, is not in the direction of the acceleration of the body. The external force F_e applied to the body to translate it through the fluid has to be applied in a direction different from that of the acceleration of the body through the fluid. Physical conditions that should be satisfied on given boundaries of the fluid (boundary conditions) depend on the assumptions made with regard to the nature of the fluid, more specifically on the nature of the differential equations that are assumed to govern the motion of the fluid. For a solid-fluid boundary, at each point of the solid-fluid surface, at every instant, the component normal to the surface of the relative velocity between the fluid and the solid must be vanish, $\vec{V} \cdot \vec{n} = 0$, where $\vec{V}$ represents the relative velocity and $\vec{n}$ the normal to the surface (fig. 4).

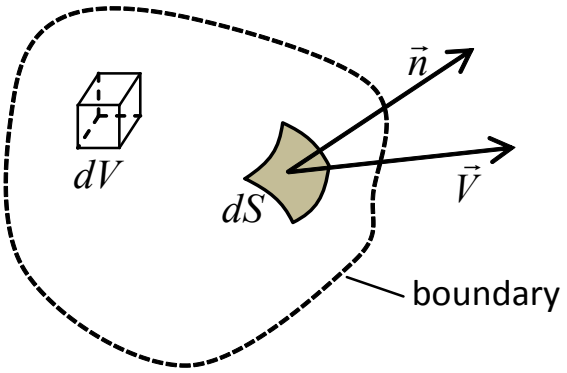

Fig. 4 Solid-fluid surface

If the surface is represented by a scalar function of position and time, $F(\vec{r},t)=0$, then the total time rate of change is zero,

$$\frac{D(F)}{Dt} = \frac{\partial(F)}{\partial t} + \vec{V} \cdot grad(F) = 0 \tag{5}$$

on $F(\vec{r},t)=0$.

The fluid force acting on a rigid body of arbitrary shape translating with a velocity $\vec{U}(t)$ is given by

$$\vec{F} = -\int_S p\,\vec{n}\,d\,S \tag{6}$$

where S denotes the surface of the body and p is the pressure on the surface of the body. In general, the body may be translating, rotating and deforming; consequently, the velocity U is a function of position on the surface and time. If the body is rigid and is in translation motion, then U is a function of time, but uniform over the surface of the body. The mathematical problem is to determine the externally force $\vec{F}_e$ applied to the body to translate it through the fluid.

According to Newton's second law, we have

$$\frac{d}{dt}\left(m\vec{U}\right) = \vec{F}_e + \vec{F} \tag{7}$$

where m is the mass of the body. The above equation may be rewritten as

$$\vec{F}_e = \frac{d}{dt}\left(m\vec{U}\right) - \vec{F} \tag{8}$$

or

$$\vec{F}_e = \frac{d}{dt}\left(m\vec{U} + \vec{I}\right) \tag{9}$$

where $\vec{I}$ is the impulse applied on the fluid and $\vec{F} = -d\vec{I}/dt$.

The fluid force acting on the body is

$$\vec{F} = \frac{\partial}{\partial t}\oint_S \rho\phi\vec{n}\,dS - \rho\vec{U}\times\oint_S \vec{n}\times grad(\phi)\,dS \tag{10}$$

The integral $\vec{I}_C = \oint_S \vec{n}\times grad(\phi)\,dS$ is related to the circulation C around the body (fig. 5) and ϕ is the potential of velocity.

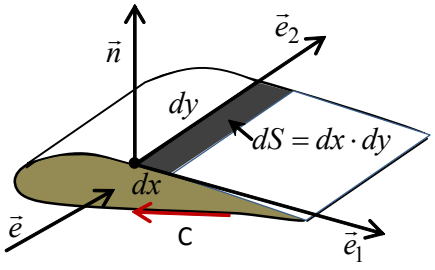

Fig. 5 Rotor blade element

The unit vector $\vec{e}$ is normal to the cutting planes, the unit vector $\vec{e}_1$ is tangent to the curve of intersection between the blade element surface and the cutting plane and the unit vector $\vec{e}_2$ is tangent to the blade element surface.

The component of the vector $\vec{I}_C$ in the direction $\vec{e}$ is

$$\vec{e}\cdot\vec{I}_C = \oint_S \vec{e}\cdot\vec{n}\times\vec{q}\,dS \tag{11}$$

and the vector $\vec{n}\,dS$ corresponding to the surface element $dS = dx\cdot dy$ may be written $\vec{n}\,dS = \overrightarrow{dx}\times\overrightarrow{dy}$, where $\overrightarrow{dx} = dx\vec{e}_1$, and $q = grad(\phi)$.

On the other hand,

$$\vec{n}\,dS\times\vec{q} = \left(\overrightarrow{dx}\times\overrightarrow{dy}\right)\times\vec{q} = \left(\vec{q}\cdot\overrightarrow{dx}\right)\overrightarrow{dy} - \left(\vec{q}\cdot\overrightarrow{dy}\right)\overrightarrow{dx}$$

and

$$\vec{e}\cdot\vec{n}\times\vec{q}\,dS = \vec{e}\left(\vec{q}\cdot\overrightarrow{dx}\right)\overrightarrow{dy} - \vec{e}\left(\vec{q}\cdot\overrightarrow{dy}\right)\overrightarrow{dx} \tag{12}$$

Since the unit vectors $\vec{e}$ and $\vec{e}_1$ are normal it follows that $\vec{e}\cdot\overrightarrow{dx} = 0$ and

$$\vec{e}\cdot\left(\vec{n}\times\vec{q}\right)dS = \left(\vec{q}\cdot\overrightarrow{dx}\right)\left(\vec{e}\cdot\overrightarrow{dy}\right) \tag{13}$$

The scalar product $\vec{e}\cdot\overrightarrow{dy}$ is the normal distance between the cutting planes of the solid body (fig. 5). If we denote $dh = \vec{e}\cdot\overrightarrow{dy}$ it follows

$$\vec{e}\cdot\oint_S \vec{n}\times\vec{q}\,dS = \int_{h_1}^{h_2}\left(\oint_C \vec{q}\cdot\overrightarrow{dx}\right)dh = \int_{h_1}^{h_2}\Gamma_e(h)\,dh \tag{14}$$

Here h is the distance measured along the fixed direction $\vec{e}$ and

$$\Gamma_e(h) = \oint_C \vec{q}\cdot\overrightarrow{dx} \tag{15}$$

is the circulation around the curve of intersection between the body surface and the cutting plane. The limits h_1 and h_2 denote the extremities of the body measured along the direction $\vec{e}$. It follows that for motions without circulation the force on the body is given by

$$\vec{F} = \frac{\partial}{\partial t}\left(\oint_S \rho\phi\vec{n}\,dS\right) \tag{16}$$

where the velocity potential ϕ is the solution of the system

$$\begin{cases}\nabla^2\phi = 0\\ grad\phi\cdot\vec{n} = \dfrac{\partial\phi}{\partial n} = U(t)n \quad on\ S\end{cases} \tag{17}$$

Since the equation and boundary condition for ϕ are linear, the solution could have the form

$$\phi = \phi_1 + \phi_2 + \phi_3 \tag{18}$$

where each of the function ϕ_1, ϕ_2 and ϕ_3 is a solution of the equations

$$\begin{cases}\nabla^2\phi_i = 0\\ grad(\phi_i)\cdot\vec{n} = \dfrac{\partial\phi_i}{\partial n} = u_i n_i \quad on\ S\end{cases} \tag{19}$$

i=1, 2 or 3.

In the Cartesian coordinate system the vectors $\vec{U}$ and $\vec{n}$ have the expressions

$$\begin{aligned}\vec{U} &= u_1\vec{i} + u_2\vec{j} + u_3\vec{k}\\ \vec{n} &= n_1\vec{i} + n_2\vec{j} + n_3\vec{k}\end{aligned} \tag{20}$$

Because time enters through u_i, it is convenient to set $\phi_i = u_i\varphi_i$, so the system (19) takes the form

$$\begin{cases}\nabla^2\varphi_i = 0\\ grad(\varphi_i)\cdot\vec{n} = \dfrac{\partial\varphi_i}{\partial n} = n_i \quad on\ S\end{cases} \tag{21}$$

With these considerations the impulse $\vec{I}$ becomes

$$-\vec{I}=\oint_S \rho\phi\vec{n}\,dS=\oint_S \rho\left(\sum_{k=1}^{3}u_k\varphi_k\right)\vec{n}\,dS=$$
$$=\sum_{k=1}^{3}\left(\oint_S \rho\varphi_k\vec{n}\,dS\right)u_k \tag{22}$$

The components of the impulse $\vec{I}=I_1\vec{i}+I_2\vec{j}+I_3\vec{k}$ are

$$\begin{cases} I_1=\vec{i}\cdot\vec{I}=\sum_{k=1}^{3}\left(-\oint_S \rho\varphi_k n_1\,dS\right)u_k \\ I_2=\vec{j}\cdot\vec{I}=\sum_{k=1}^{3}\left(-\oint_S \rho\varphi_k n_2\,dS\right)u_k \\ I_3=\vec{k}\cdot\vec{I}=\sum_{k=1}^{3}\left(-\oint_S \rho\varphi_k n_3\,dS\right)u_k \end{cases} \tag{23}$$

The surface integral in the above equations may be written as follows

$$\oint_S \rho\varphi_k n_i\,dS=\oint_S \rho\varphi_k\frac{\partial\varphi_i}{\partial n}dS \tag{24}$$

According to Green's theorem, if ψ_1 and ψ_2 are two harmonic functions, then

$$\oint_S \psi_1\frac{\partial\psi_2}{\partial n}dS=\oint_S \psi_2\frac{\partial\psi_1}{\partial n}dS \tag{25}$$

Introducing the symbol m_{ki},

$$m_{ki}=-\oint_S \rho\varphi_k\frac{\partial\varphi_i}{\partial n}dS \tag{26}$$

with $m_{ki}=m_{ik}$, the components of the impulse $\vec{I}$ are therefore given by

$$I_i=\sum_{k=1}^{3}m_{ik}u_k \quad \text{, i=1, 2, 3} \tag{27}$$

and the force applied externally to the body is

$$\vec{F}_e=\frac{d}{dt}m\left(u_1\vec{i}+u_2\vec{j}+u_3\vec{k}\right)+$$
$$+\frac{d}{dt}\left(m_{11}u_1+m_{12}u_2+m_{13}u_3\right)\vec{i}+$$
$$+\frac{d}{dt}\left(m_{11}u_1+m_{12}u_2+m_{13}u_3\right)\vec{j}+$$
$$+\frac{d}{dt}\left(m_{11}u_1+m_{12}u_2+m_{13}u_3\right)\vec{k} \tag{28}$$

or

$$\vec{F}_e=\left[\left(m+m_{11}\right)\frac{du_1}{dt}+m_{12}\frac{du_2}{dt}+m_{13}\frac{du_3}{dt}\right]\vec{i}+$$
$$+\left[m_{21}\frac{du_1}{dt}+\left(m+m_{22}\right)\frac{du_2}{dt}+m_{23}\frac{du_3}{dt}\right]\vec{j}+$$
$$+\left[m_{31}\frac{du_1}{dt}+m_{32}\frac{du_2}{dt}+\left(m+m_{33}\right)\frac{du_3}{dt}\right]\vec{k}$$

The coefficients m_{ik} form a set of nine numbers which may be displayed as an array

$$\begin{pmatrix} m_{11} & m_{12} & m_{13} \\ m_{21} & m_{22} & m_{23} \\ m_{31} & m_{32} & m_{33} \end{pmatrix} \tag{29}$$

which may be referred to as a virtual mass tensor or virtual masses that need to be added to the mass of the body in order to find the force that must be applied to translate it through the fluid. Introducing the symbol δ_{ik} defined by $\delta_{ik}=0$ if $i\neq k$ and $\delta_{ik}=1$ for $i=k$, equation (28) may be rewritten

$$\left(F_e\right)_i=\sum_{k=1}^{3}\left(m\delta_{ik}+m_{ik}\right)\frac{du_k}{dt} \tag{30}$$

For any body there are three perpendicular directions such that $m_{ik}=0$ for $i\neq k$, so with respect to such axes, the equation (30) becomes

$$\left(F_e\right)_i=\left(m+m_{ii}\right)\frac{du_i}{dt} \quad \text{, i=1, 2, 3.} \tag{31}$$

The sum $\left(m+m_{ii}\right)$ represents the apparent mass for translation in the i-direction and the corresponding m_{ii} is the additional apparent mass.

3. RESULTS

The oscillatory motion of the airfoil can be decomposed into contributions associated with angle of attack which is equivalent to a pure plunging motion (fig. 6) and contributions associated with pitching (fig. 7).

A plunge velocity $\dot{h}$ produces a uniform velocity perturbation w, that is normal to the chord, $w(x)=-\dot{h}$ and the pitch-rate term produces a linear variation in normal perturbation velocity.

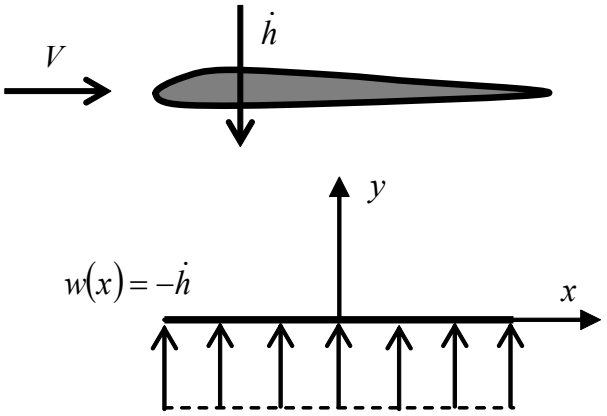

Fig. 6 Plunge velocity

For a pitch rate imposed about an axis at "*a*" semi-chords from the mid-chord, then $w(x) = -\dot{\alpha}(x-a)$ so that the induced chamber is a parabolic arc.

The problem of finding the air loads on an oscillating airfoil was solved by Theodorsen, who gave a solution to the unsteady air loads on a 2-D harmonically oscillated airfoil in inviscid, incompressible flow, with the assumption of small disturbances. Both the airfoil and its shed wake were represented by a vortex sheet with the shed wake extending as a planar surface from the trailing edge downstream to infinity. The assumption of planar wake is justified if the angle of attack disturbances remain relatively small. As with the standard quasi-steady thin airfoil theory, the bound vorticity, γ_b, can sustain a pressure difference and, therefore, a lift force.

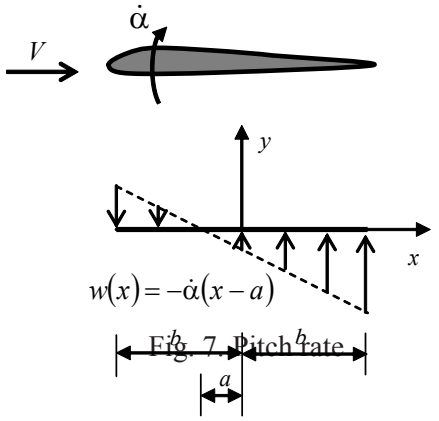

Fig. 7 Pitch rate

The wake vorticity, γ_w, must be force free with zero net pressure jump over the sheet.

According to the Theodorsen's theory, the solution for the loading γ_b on the airfoil surface under harmonic forcing conditions is obtained from integral equation

$$w(x,t) = \frac{1}{2\pi}\int_0^c \frac{\gamma_b(x,t)}{x-x_0}dx + \frac{1}{2\pi}\int_c^\infty \frac{\gamma_w(x,t)}{x-x_0}dx \tag{32}$$

where *w* is the downwash on the airfoil surface.

At the trailing edge, $\gamma_b(c,t) = 0$, and the airfoil circulation $\Gamma(t)$ is given by

$$\Gamma(t) = \int_0^c \gamma_b(x,t)dx \tag{33}$$

So long as the circulation about the airfoil is changing with respect to time, the circulation is continuously shed into the wake and will continuously affect the aerodynamic loads on the airfoil. For a general motion, where an airfoil of chord $c = 2b$ is undergoing a combination of pitching $(\alpha, \dot{\alpha})$ and plunging $(\dot{h})$ motion in a flow of steady velocity *V,* Theodorsen's solutions for the lift coefficient and pitching moment coefficient corresponding to mid-chord, $M_{1/2}$ are

$$\begin{cases} c_l = \pi b\left[\dfrac{\ddot{h}}{V^2} + \dfrac{\dot{\alpha}}{V} - \dfrac{b}{V^2}a\ddot{\alpha}\right] + \\ \quad + 2\pi\left[\dfrac{\dot{h}}{V} + \alpha + \dfrac{b\dot{\alpha}}{V}\left(\dfrac{1}{2}-a\right)\right]C(k) \\ c_{m1/2} = \dfrac{\pi}{2}\left[\dfrac{b}{V^2}\ddot{h} - \dfrac{b^2}{V^2}\left(\dfrac{1}{8}+a^2\right)\ddot{\alpha}\right] + \\ \quad + \pi\left(a+\dfrac{1}{2}\right)\left[\dfrac{\dot{h}}{V} + \alpha + b\left(\dfrac{1}{2}-a\right)\dfrac{\dot{\alpha}}{V}\right]C(k) - \\ \quad - \dfrac{\pi}{2}\left[\left(\dfrac{1}{2}-a\right)\dfrac{b\dot{\alpha}}{V}\right] \end{cases}$$

where *a* is the pitch axis location relative to the mid-chord of the airfoil, measured in terms of semi-chord and $C(k) = F(k) + iG(k)$ is the complex transfer function. It could be appreciated that $C(k)$ function serves to introduce an amplitude reduction and phase lag effect on the circulatory part of the lift response compared to the result obtained under quasi-steady conditions [3].

This effect can be seen if a pure oscillatory variation in angle of attack is considered, that is, $\alpha = \bar{\alpha} e^{i\omega t}$, so the circulatory part of the airfoil lift coefficient is given by

$$c_l = 2\pi\bar{\alpha} C(k) = 2\pi\bar{\alpha}\left[F(k) + iG(k)\right] \tag{34}$$

For $k = 0$, the steady-state lift behavior is obtained, that is, c_l is linearly proportional to α. As k is increased, the lift plots develop into hysteresis loops and these loops rotate such that the amplitude of the lift response (half of the peak-to-peak value) decreases with increasing reduced frequency. These loops are circumvented in a counterclockwise direction such that the lift is lower than the steady value when α is decreasing with time (i.e., there is a phase lag). For infinite reduced frequency the circulatory part of the lift amplitude is half that at $k = 0$ and there is no phase lag angle. The noncirculatory or apparent mass terms arise from the velocity gradient term and account for the pressure forces required to accelerate the fluid in the vicinity of the airfoil.

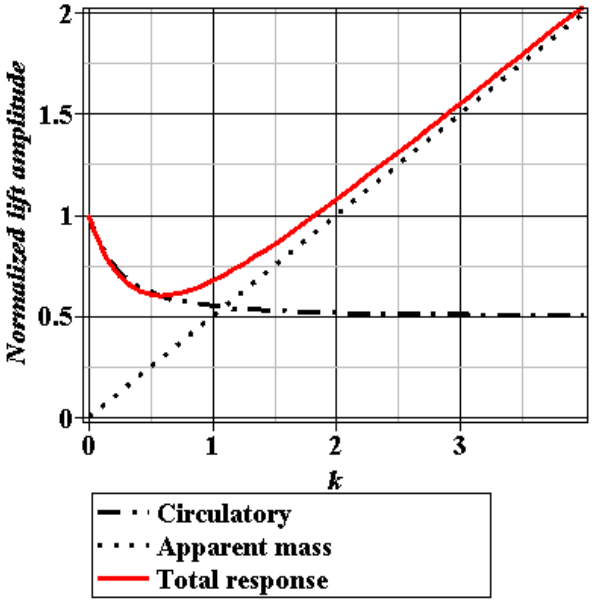

Fig. 8 Normalized lift amplitude

The normalized lift amplitude, $c_l / 2\pi\alpha$ and phase of lift for pure angle of attack oscillations are presented in fig. 8 and fig. 9, where the significance of the apparent mass contribution to both the amplitude and phase can be appreciated.

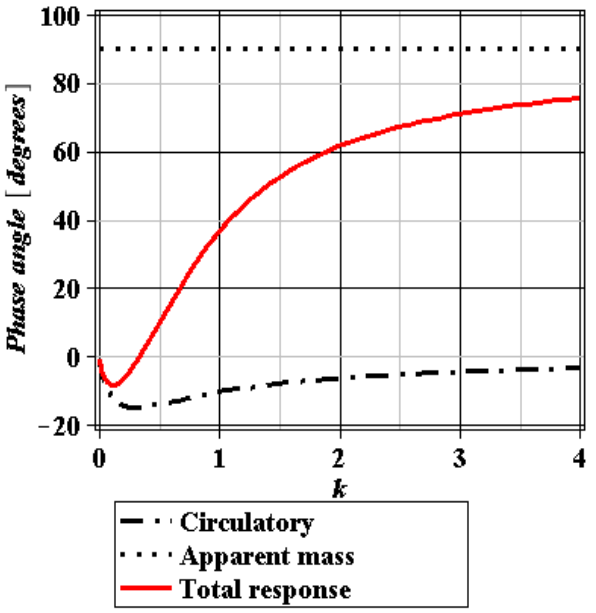

Fig. 9 Phase angle

At lower values of reduced frequency, the circulatory terms dominate the solution. At higher values of reduced frequency, the apparent mass forces dominate.

For harmonic pitch oscillations, additional terms involving pitch rate $\dot{\alpha}$ appear in the equations for the aerodynamic response. The forcing is given by $\alpha = \bar{\alpha} e^{i\omega t}$ and the pitch rate by $\dot{\alpha} = i\omega\bar{\alpha} e^{i\omega t}$. In this case, the lift coefficient is

$$c_l = 2\pi\left[F(1+k) + G(i-k)\right]\bar{\alpha} e^{i\omega t} + \pi k\left(i - \frac{k}{2}\right)\bar{\alpha} e^{i\omega t} \tag{35}$$

The lift amplitude initially decreases with increasing k because of the effects of the shed wake and then, for $k > 0.5$ begins to increase, as the apparent mass forces begin to dominate the air loads.

4. CONCLUSIONS

The airfoil can generate high lift as a result of a vortex that is shed at the leading edge at the instant of stall. The vortex travels back over the top of the airfoil carrying with it a low pressure wave that accounts for the very large lift coefficient.

When a wing's angle of attack is increased rapidly, it can momentarily generate a higher maximum lift coefficient than it could if the angle of attack were increased slowly. This overshoot can be related to the change in angle of attack during the time required for the air to travel one chord length. The dynamic overshoot is attributed to two effects (for the airfoils that stall first at the leading edge): the delay in the separation of the boundary layer and the momentary existence of a vortex shed at the leading edge after the boundary layer does separate. The delay in separation corresponds to the finite time required for the aft edge of the separation bubble to move forward to its bursting position. Airfoils that stall first at the trailing edge also exhibit a dynamic overshoot, but considerably less than those airfoils that have leading edge stall.

BIBLIOGRAPHY

1. Gareth, D. Padfield, (2007). *Helicopter Flight Dynamics,* AIAA Education Series.
2. Gordon Leishman, (2007). *Principles of Helicopter Aerodynamics,* Cambridge University Press.
3. Prouty, R. (2002). *Helicopter Performance,Stability and Control,* Krieger Publishing Company, Florida, USA.
5. Rotaru, C., Circiu, I., Boscoianu M. (2010). *Computational Methods for the Aerodynamic Design*, Review of the Air Force Academy, No 2(17), p. 43-48.
6. Rotaru,C., Jaulin, V., Monot, V. (2012). *Aspects regarding the nonsteady aerodynamics and its applications to helicopter rotor blade*, International Conference AFASES, Braşov, Romania.
7. Rotaru, C., Arghiropol A. (2010). *Maple soft solutions for nonlifting flows over arbitrary bodies,* Proceedings of the 3rd WSEAS international conference on FINITE DIFFERENCES - FINITE ELEMENTS - FINITE VOLUMES - BOUNDARY ELEMENTS, ISSN 1970-2769, p. 270-274.
8. Sedon, J., Newman, B. (2001). *Basic Helicopter Aerodynamics,* AIAA Education Series.